JOURNAL OF SOLID STATE CHEMISTRY **44**, 60–74 (1982)

Crystallographic Shear in the Nb_2O_5–WO_3 and Ta_2O_5–WO_3 Systems*

P. J. ENGLAND, J. BOOTH,† AND R. J. D. TILLEY

School of Materials Science, University of Bradford, Bradford BD7 1DP,
West Yorkshire, U.K.

AND THOMMY EKSTRÖM

Department of Inorganic Chemistry, Arrhenius Laboratory, University of
Stockholm, S 106 91 Stockholm, Sweden

Received October 26, 1981

Crystallographic shear (*CS*) phases occurring in the Nb_2O_5–WO_3 and Ta_2O_5–WO_3 systems near to WO_3 were characterized by X-ray diffraction and high-resolution transmission electron microscopy. The Nb_2O_5–WO_3 samples were heated at 1600K. They contained ordered {104} and {001} *CS* planes and wavy *CS* which were composed of intergrowths of {104} and {001} *CS* segments. The composition range over which the {104} *CS* series extended was from $(Nb,W)O_{2.954}$ i.e., $(Nb,W)_{65}O_{192}$, to $(Nb,W)O_{2.942}$, i.e., $(Nb,W)_{52}O_{153}$. The composition range over which the {001} *CS* series extended was from $(Nb,W)O_{2.9375}$, i.e., $(Nb,W)_{16}O_{47}$ to $(Nb,W)O_{2.875}$, i.e., $(Nb,W)_8O_{23}$. The Ta_2O_5–WO_3 samples were prepared at 1593, 1623, and 1672K. At lower temperatures ordered {103} *CS* phases were found, with a composition range extending between $(Ta,W)O_{2.960}$, i.e., $(Ta,W)_{50}O_{148}$, to $(Ta,W)O_{2.944}$, i.e., $(Ta,W)_{36}O_{106}$. At 1673K ordered {103} *CS* phases occurred, as did wavy *CS* composed of intergrowths of {103} and {104} *CS* segments.

Introduction

When tungsten trioxide is reacted with either Nb_2O_5 or Ta_2O_5 a number of interesting compounds are formed. At low temperatures the phase region near to WO_3 is of the tetragonal tungsten bronze (*TTB*) type and contains pentagonal column (*PC*) units as the major structural motif. At higher temperatures crystallographic shear (*CS*) phases are found. In order to try to understand the factors that determine which of these two structure types are formed we investigated the structures formed in both of these systems at a number of temperatures. In a previous report, the phase relations for the Nb–W–O and Ta–W–O systems at about 1373K were described (*1*). At this temperature it was found that the lowering of the oxygen-to-metal ratio was achieved by interpolation of *PC*s into the WO_3 matrix. These were often disordered, especially for compositions close to WO_3. *CS* phases, when present, were found only for compositions close to the W–O line of the phase diagram and were not believed to contain appreciable amounts of either tantalum or niobium.

---

* Dedicated to Professor A. F. Wells on his 70th birthday.

† Present address: ICI Corporate Laboratory, P.O. Box 11, The Heath, Runcorn, Cheshire, U.K.

0022-4596/82/100060-15$02.00/0

Copyright © 1982 by Academic Press, Inc.
All rights of reproduction in any form reserved.

This is in contrast to the situation reported at higher temperatures. For example, a detailed study of the Nb_2O_5–WO_3 system by Roth and Waring (*2*) using X-ray methods indicated the existence of a *CS*-phase region lying between 91 to 94 mole% WO_3 at temperatures above about 1548K. Electron microscope studies on these *CS* phases have given a more detailed picture of the microstructures which are produced than X-ray methods permit. Allpress (*3*) investigated preparations in the system containing between 3 and 9 mole% Nb_2O_5 and found two series of *CS* phases. At higher niobium concentrations the *CS* planes lie parallel to {001} and at somewhat lower niobium concentrations, parallel to {104}. In addition some {102} *CS* planes were found at the lowest niobium concentrations. Bursill and Hyde (*4*) studied a similar phase region in the Nb_2O_5–WO_3 system and confirmed these results. They also found evidence for the existence of {105} *CS* planes.

There is less information available for the Ta_2O_5–WO_3 *CS* region. Magnéli and coworkers (*5, 6*) in some powder X-ray diffraction studies identified a *CS* phase of composition $Ta_4W_{35}O_{115}$ with *CS* planes parallel to {103}. The only electron microscope study reported to date is that of Bursill and Hyde (*4*), who briefly examined some Ta_2O_5–WO_3 samples which were close in composition to WO_3 and found only {103} *CS* phases. In addition, a small amount of additional material on *CS* in the Nb_2O_5–WO_3 and Ta_2O_5–WO_3 systems, and comparisons with *CS* in WO_{3-x}, will be found in recent reviews by Ekström and Tilley (*7*) and Tilley (*8*).

These earlier studies, although not detailed enough to provide a perfect picture of these systems, show that in the composition region close to WO_3 the Ta_2O_5–WO_3 system behaves differently to the Nb_2O_5–WO_3 system at higher temperatures. However, no careful study utilizing high-resolution electron microscopy exists of these two systems and the limits of the *CS* regions are not known with any degree of precision. The present paper begins to fill this gap by reporting the results of a study of both the Nb_2O_5–WO_3 and the Ta_2O_5–WO_3 systems for the composition region near to WO_3. The results are compared with those found at lower temperatures (*1*) and discussed in terms of the known crystal chemistry of *CS* and related structures.

Experimental

The starting materials for the Nb_2O_5–WO_3 samples were Nb_2O_5 and WO_3 (Johnson Matthey, specpure grade). Appropriate weighed mixtures of Nb_2O_5 and WO_3 were sealed in platinum tubes without grinding or premixing and these were sealed in evacuated silica ampoules. This specimen preparation technique assured chemical inhomogeneity and avoided an approach to true equilibrium. They were then heated for between 40 hr and 20 days at 1600K. Following heat treatment the samples were removed from the furnace and allowed to cool in air.

For Ta_2O_5–WO_3 specimens the starting materials were Ta_2O_5 and WO_3 (Johnson Matthey, specpure grade). Appropriate amounts of these chemicals were weighed and mixed by grinding under methanol (Analar grade) in an agate mortar. The resulting slurry was dried at 50°C and then sealed into platinum tubes, which were heated at 1623 or 1673K for 5 days. After heating, the tubes were quenched by dropping them into liquid nitrogen. A further series of Ta_2O_5–WO_3 samples, for X-ray analysis, were prepared by heating mixtures of Ta_2O_5 and WO_3 for 11 days at 1593K. This specimen preparation technique was used here in an attempt to approach equilibrium.

The samples were examined by optical microscopy under polarized light using a Zeiss Ultraphot microscope, and by electron microscopy using a JEM 100B electron microscope fitted with a goniometer stage and operated at 100 kV. The electron microscope specimens were prepared by grinding the material in an agate mortar under *n*-butanol and allowing a drop of the resultant suspension to dry on a perforated carbon support film. High-resolution micrographs were taken of thin edges of suitably oriented fragments which projected over holes in the support film. All samples were investigated by recording their X-ray powder patterns at room temperature in a Guinier–Hägg focusing camera using $CuK\alpha_1$ radiation and KCl ($a = 0.6293$ nm) as an internal standard. In addition, a few selected samples were chosen for careful diffractometry measurement. In the latter case the spectra were recorded in a step scan mode (0.01° in 2θ per step) using Cu radiation.

Some samples were analyzed by X-ray emission analysis using a JEOL JSM 35 scanning electron microscope or an ISI Super IIIA scanning electron microscope fitted with X-ray analysis equipment.

Results

The Nb_2O_5–WO_3 System

Optical examination of the samples after firing showed considerable variation in crystal habit in all preparations, suggesting that equilibrium had not been reached, even after 20 days heating. This was subsequently confirmed by the electron microscope results reported below. The preparations were found to consist of rather chunky columnar crystals of a green or lemon yellow color and very fine pale yellow to white needles in the form of a tangled wool. These two crystal habits were frequently separated in the preparation tubes, but sometimes columnar crystals could be found with the woolly material or vice versa. Careful optical examination allowed these two broad types of crystals to be further subdivided but detailed optical classification was not carried out.

Electron microscopy revealed that the columnar or chunky crystals were *CS* phases and no significant difference in the microstructures of the more green or more yellow crystals was detected. The very fine wool-like needle compacts proved to be *TTB* phases, a result confirmed by X-ray powder diffraction. The structures found are listed in Table 1 and summarized in Fig. 1. Some features of the results are discussed in the sections which follow.

{001} CS Phases

Examination by electron microscopy revealed that the most commonly occurring *CS* structure found was the {001} type, which was present in all but one of our preparations. Electron micrographs showed that these materials were generally well ordered, as shown in Fig. 2, but images obtained at high resolution sometimes revealed small irregularities in the spacing of *CS* planes. No changes were observed in the degree of ordering of the *CS* planes when samples heated for only 40 hr were compared to those heated for 10 or 20 days.

In order to analyze the distribution of *CS* plane spacings in the samples, about 60 crystal fragments were aligned and their diffraction patterns were recorded for each composition prepared. The diffraction patterns from such materials, a typical example of which is shown in Fig. 2b, consist of a set of intense WO_3 subcell reflections separated by superlattice spots. These can be used to calculate the value of *n* in the series

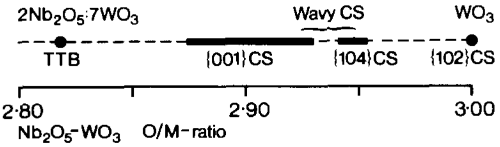

FIG. 1. Schematic illustration of structures found in the tungsten trioxide-rich part of the Nb_2O_5–WO_3 system at 1600K.

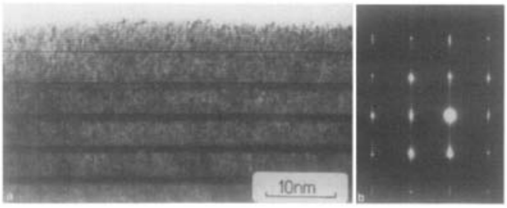

FIG. 2. (a) Electron micrograph of a crystal fragment of a well-ordered {001} *CS* phase from a sample of overall composition $1Nb_2O_5:8WO_3$. Note that the *CS* plane images lose sharpness as the crystal thickness increases, away from the crystal edge. (b) Diffraction pattern from the crystal, showing an intense square array of subcell spots, corresponding to the WO_3-like matrix, and superlattice spots, along [001], indicative of the *CS* plane spacing.

formula $(Nb,W)_nO_{3n-1}$, which describes these oxides, following the analysis of Bursill and Hyde (*4*). These surveys showed that there were no significant changes in the distribution of n values in samples heated for 40 hr compared to those heated for 10 or 20 days. In Figs. 3a and b we show the distribution of n values for the samples of overall compositions $(Nb,W)O_{2.90}$ and $(Nb,W)O_{2.925}$ which contain the accumulation of all of the data for each of the compositions. Thus Fig. 3a contains the total data for the two $(Nb,W)O_{2.90}$ samples heated for 40 hr and 10 days at 1600K, while Fig. 3b contains the total data for the three $(Nb,W)O_{2.925}$ samples heated for 40 hr, 10 days, and 20 days. The figures indicate that there is no strong preference for one n value compared to another in our preparations, although it must be noted that n values of 8, 9, and 16 were only rarely encountered in this study. From this data we can conclude that the maximum phase range of the {001} *CS* structures at temperatures close to 1600K is from $(Nb,W)O_{2.9375}$ to $(Nb,W)O_{2.875}$, i.e., $(Nb,W)_{16}O_{47}$ to $(Nb,W)_8O_{23}$.

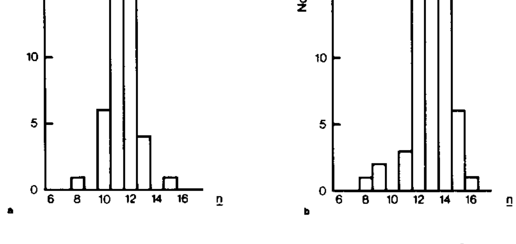

FIG. 3. Histograms showing the occurrence of crystal fragments with a given value of n in the formula $(Nb,W)_nO_{3n-1}$, for {001} *CS* structures in samples of overall composition (a) $(Nb,W)O_{2.90}$ and (b) $(Nb,W)O_{2.925}$.

The electron microscope results are substantiated by the powder X-ray diffraction results. In samples of gross composition $(Nb,W)O_{2.90}$ usually only {001} *CS* structures were identified, although occasionally very weak diffraction lines of the *TTB* structure $2Nb_2O_5:7WO_3$ were seen. The lower phase limit of the {001} *CS* structure field would be about or just lower than $(Nb,W)O_{2.90}$. Similarly the X-ray diffraction analysis of $(Nb,W)O_{2.925}$ shows the major crystal component to be the {001} *CS* type. A precise upper phase limit of the {001} *CS* field is not easily established by the use of X-ray diffraction because of the similarity of the different *CS* structures, and the fact that disordered structures such as "wavy *CS*" will not produce very distinct X-ray diffraction patterns. However, the general appearance of an {001} *CS* pattern can usually be distinguished from other *CS* types, and from an X-ray point of view it proved reasonable to assign the {001} *CS* field the extension $MO_{2.90}$–$MO_{2.93}$, although indexing of such patterns presents considerable difficulties in multiphasic or nonequilibrium samples (*9, 10*).

{104} CS Phases

Well-ordered arrays of {104} *CS* planes were found in the $(Nb,W)O_{2.925}$ and

TABLE 1

STRUCTURES FOUND IN Nb_2O_5–WO_3 PREPARATIONS

Sample details			Electron microscopy[a]						
Metal: oxygen ratio	Preparation time (hr) at 1600K	Optical microscopy	*TTB*	{001} *CS*	{104} *CS*	Wavy *CS*	{102} *CS*	WO_3	X-Ray powder diffraction
$MO_{2.85}$	72	Dark yellow, chunky		17		3			$2Nb_2O_5:7WO_3$, {001} *CS*
		Yellow, needle-like	1						
		Green, needle-like	16						
		Pale green, needle-like	2				1		
$MO_{2.90}$	40	Yellow, chunky		18					{001} *CS*
		Green, chunky		17					
$MO_{2.90}$	240	Pale yellow, needle-like	2						{001} *CS*, v. weak $2Nb_2O_5:7WO_3$
		Yellow, chunky		17					
		Green, chunky		18					
$MO_{2.925}$	40	Green, chunky		9	4	1		2	{001} *CS*, v. weak WO_3, v. weak {104} *CS*
		Yellow, chunky		9	2	4			
$MO_{2.925}$	240	Pale yellow, needle-like	2						{001} *CS*, {104} *CS*
		Yellow, chunky		3	3	9			
		Dark yellow, chunky		12	1			3	
$MO_{2.925}$	480	Pale green, needle-like		12	2	1			{001} *CS*, weak {104} *CS*, v. weak WO_3
		Yellow-green, chunky		18		3			
		Dark green, chunky		5	14	4	2	5	
$MO_{2.95}$	72	Dark yellow, chunky			2	1	1	18	{104} *CS*, weak WO_3
		Yellow, chunky		3	1	11			
		Green, chunky					8	8	
		Pale green, needle-like	4	3		1			

[a] The number of fragments of a given structure type examined are recorded. *TTB* refers to samples with a variant of the tetragonal tungsten bronze structure.

$(Nb,W)O_{2.95}$ preparations, but not in those of $(Nb,W)_{2.85}$ or $(Nb,W)O_{2.90}$. As this *CS* type was present in samples heated for 20 days at 1623K it is clear that these phases do not decompose rapidly or have a transient existence. Electron micrographs of these crystals, an example of which is shown in Fig. 4, reveal that the spacings between the *CS* planes vary and also that the blocks of edge-sharing octahedra which make up the *CS* plane vary in size, and are not always made up of eight linked MO_6 octahedra.

Ordered {104} *CS* planes give rise to a homologous series with the compositions of the members given by the series formula $(Nb,W)_nO_{3n-3}$. The value of the integer n can be determined from the diffraction patterns (*4*), but in this case the values obtained can be considered as only approximate. This is because the superlattice spots lying along the [104] directions are closely spaced and also extend for only a short distance to either side of the WO_3 sublattice reflections, as can be seen from the diffraction pattern illustrated in Fig. 4. With this limitation in mind, the range of n values occurring in our preparations was found to be from 52 to 65, which corresponds to composition limits of $(Nb,W)O_{2.942}$ to $(Nb,W)O_{2.954}$. The frequency of occurrence of each n value is shown in the histogram in Fig. 5, from which it is seen that values less than 54 or greater than 60 were only rarely encountered.

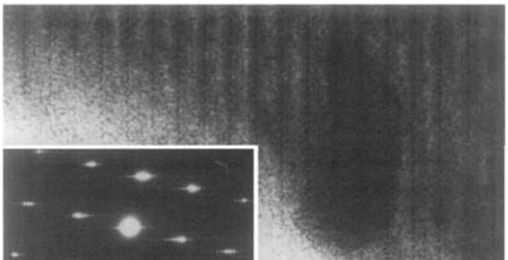

FIG. 4. (a) Electron micrograph of a crystal fragment of a well-ordered {104} *CS* phase, from a sample of overall composition $0.075\ Nb_2O_5 : 0.85WO_3$. Examination of the *CS* planes shows that not all the blocks of edge-sharing octahedra are identical. (b) Inset is the diffraction pattern from the crystal, showing that the superlattice spots only extend a short distance from the subcell array.

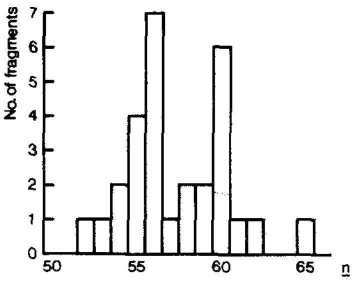

FIG. 5. Histogram showing the occurrence of crystal fragments with a given value of n in the formula $(Nb,W)_nO_{3n-3}$, for {104} *CS* structures.

As found for the {001} *CS* structure field, the X-ray powder patterns of $(W,Nb)O_{2.95}$ varied somewhat from one preparation to another. The general appearance could, though, be distinguished from those samples lying in the {001} *CS* field and in this way the X-ray powder patterns served as a broad indication of the presence of {104} *CS* structures, and confirmed the composition limits for this structure type found by electron microscopy.

Wavy CS Structures

At low magnifications, electron microscope images of crystals containing {001} or {104} *CS* planes show the crystal flakes to be crossed by one or more sets of parallel straight lines, which are the traces of the *CS* planes in the surface of the crystal fragment. In the $(Nb,W)O_{2.95}$ and $(Nb,W)O_{2.925}$ preparations a number of crystal fragments were found in which these lines were wavy, as shown in Fig. 6. Similar *CS* surfaces have also been observed by Allpress (*3*) and Bursill and Hyde (*4*). In our preparations, these wavy *CS* structures were by no means rare, as the data in Table 1 reveal.

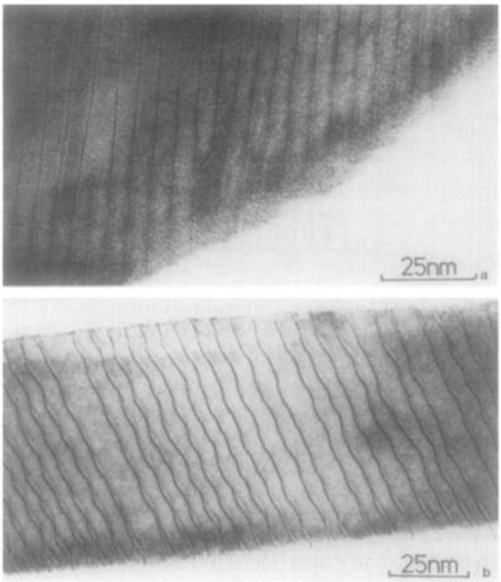

FIG. 6. Typical examples of wavy *CS* planes from WO_3–Nb_2O_5 samples. (a) shows irregular *CS* planes in a sample of composition $0.075Nb_2O_5 : 0.85WO_3$ containing an intergrowth of {104} and {103} *CS* units, while (b) shows a situation approaching a regular wave-like array, in which {001} and {104} *CS* units alternate, from a sample of overall composition $0.05Nb_2O_5 : 0.9WO_3$.

The degree of ordering of these wavy *CS* surfaces varied considerably. In some crystal fragments only small areas of irregular *CS* were seen between large regions of parallel *CS* arrays, while in other crystal fragments areas of fairly regular waves could be seen. Between these two extremes a wide variety of degrees of ordering and waveform were noted, the full range of features needing some dozen micrographs to illustrate them adequately.

At moderate and high resolution the wavy *CS* surfaces were usually found to be made up of intergrowths of segments of {001} and {104} *CS* planes, as shown in Fig. 7. The {001} segments are, as can be seen, rather short, and could be described in terms of blocks of {10m} *CS* planes, where m is an integer lying between 4 and infinity. The wave amplitude depends on the relative number of {104} units compared to {001} units, and it has been noticed that as the composition of the sample falls, the wave amplitude decreases. Disorder was also found in the {104} component of these waves and sometimes blocks with more or less than eight edge-sharing octahedra were found corresponding to units of {103}, {105} *CS* and so on.

The diffraction patterns from these crystals gave little information about the microstructural complexity of the material. Usually diffraction patterns showed arrays of spots along one or two {104} directions, exactly as obtained from ordered {104} *CS* arrays. More rarely the superlattice spots and streaks were at a small angle to {001} and one pattern had these lying along {105}. Such diffraction patterns alone should not, therefore, be taken to indicate ordered arrays of *CS* planes with indices lying in these directions without confirmation from the micrographs themselves.

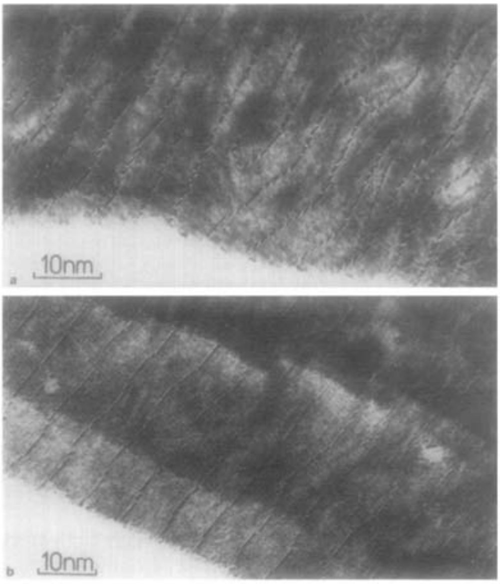

FIG. 7. (a) and (b). Examples of wavy *CS* planes, showing the variety of units of edge-sharing octahedra which are found in these structures. Both crystal fragments were from a sample of overall composition $0.05Nb_2O_5 : 0.9WO_3$.

{102} CS Planes

Crystal fragments containing disordered {102} *CS* planes similar in appearance to those found in slightly reduced WO_3 were found in *all* preparations made, which underlies the basic lack of equilibrium achieved in these samples, even when heating times of 20 days at 1600K were employed. The spacings between *CS* planes ranged from about 1.4 to about 29 nm, but ordered arrays were never encountered. As the appearance of these fragments is identical with those illustrated before for reduced WO_3 (*8*), we will not include micrographs here.

Powder X-ray diffraction does not directly reveal the presence of such irregularly spaced {102} *CS* planes. However, the presence of low concentrations of such *CS* planes seems to be able to stabilize the high-temperature orthorhombic form of WO_3 to room temperature (*1*, *9*) and we found this to be a valuable diagnostic test for the presence of {102} *CS* planes which usually produce no other X-ray evidence. In the present studies, the X-ray diffraction patterns of the WO_3 component of our preparations always revealed that both the monoclinic and orthorhombic forms of this oxide were present, although only the orthorhombic form was reported in similar compositions by Roth and Waring (*2*) in their studies. We therefore take it that a low concentration of {102} *CS* planes exists in the WO_3 found in our preparations, even in samples not checked by electron microscopy.

The Ta_2O_5–WO_3 System

Optical microscopy revealed that the samples contained two broad types of crystal habit, one being needle-like, and one rather chunky. Needle-like crystals were of pale green, yellow, or blue color, while the chunky crystals were darker yellow or green. A combination of electron microscopy and X-ray analysis showed that the needle-like crystals in most cases contained *TTB*-type phases, and that the chunky crystals contained *CS* phases. The *CS*-phase region found was dominated by {103} *CS* structures, with small amounts of {102} *CS*, and at 1673K, {104} *CS*. The details of the structures found are contained in Table 2. The individual *CS* types found are reported in more detail below and the composition ranges over which they occur are illustrated schematically in Fig. 8.

{103} CS Phases

In samples prepared at 1623K crystals containing {103} *CS* phases were found in large numbers in the $MO_{2.95}$ preparation, and to a much lesser extent in the $MO_{2.90}$ preparation. The same was true of preparations heated at 1673K. Diffraction patterns obtained from fragments containing {103} *CS* phases reflected various degrees of order; some showing streaking along {103} directions while others revealed continuous rows of superlattice spots between the WO_3-type sublattice spots. In most cases the superlattice spots extended only short distances from sublattice spots, so that the exact spacings could only be estimated. The values for n in the series formula $(Ta, W)_nO_{3n-2}$ obtained from fairly well ordered {103} *CS* phases in the $MO_{2.95}$ sample, using the method of Bursill and Hyde (*4*), varied between 43 and 50, as seen in Fig. 9a, and between 44 and 48 in the

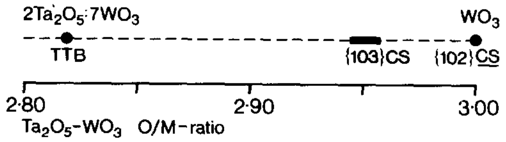

FIG. 8. Schematic illustration of structures found in the tungsten trioxide-rich part of the Ta_2O_5–WO_3 system at 1623K. At 1673K we also find the $W_{24}O_{68}$ structure type ($MO_{2.83}$) and {104} *CS* appearing in the composition region between the {103} *CS* phases and $2Ta_2O_5:7WO_3$, but the data is, as yet, insufficient to plot on the figure.

TABLE 2

STRUCTURES FOUND IN Ta_2O_5–WO PREPARATIONS

Sample details			Electron microscopy[a]							
Metal: oxygen ratio	Preparation time (hr/K)	Optical microscopy	*TTB*[b] type	$W_{24}O_{68}$ type	{104} *CS*	{103} *CS*	Wavy *CS*	{102} *CS*	WO_3	X-Ray powder diffraction
$MO_{2.975}$	120/1623	Blue-green, chunky					5	5	11	WO_3, {103} *CS*
		Yellow-green, chunky				13			2	
$MO_{2.95}$	120/1623	Yellow, needles				13			3	{103} *CS*, weak WO_3
		Yellow, chunky				16				
		Green-yellow, chunky				18				
		Green, chunky				2		2	14	
$MO_{2.90}$	120/1623	Yellow, needles	1							{103} *CS*, $2Ta_2O_5:7WO_3$
		Pale green, needles				1				
		Green, needles				4				
$MO_{2.85}$	120/1623	Green-yellow, needles								
		Pale-blue, needles	5							
$MO_{2.925}$	72/1673	Blue-green, chunky		2	1	7	4		3	$2Ta_2O_5:7WO_3$
		Yellow, needles	4	6						
$MO_{2.90}$	72/1673	Green-blue, chunky	2			4	10			
		Blue, chunky	3							
		Pale blue, needles								

[a] The number of fragments of a given structure type are recorded.

[b] *TTB* refers to samples with a variant of the tetragonal tungsten bronze structure.

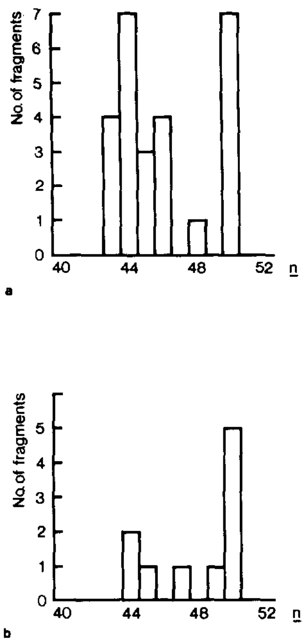

FIG. 9. Histograms showing the occurrence of crystal fragments with a given value of *n* in the formula $(Ta,W)_nO_{3n-2}$, for {103} *CS* structures in samples of overall composition (a) $(Ta,W)O_{2.95}$ and (b) $(Ta,W)O_{2.975}$.

$MO_{2.975}$ sample, as shown on Fig. 9b. Too few well-ordered crystals were found in the other preparations to allow a histogram to be drawn, but we can record that in the $(Ta,W)O_{2.90}$ sample heated at 1623K, the *n* values of the three well-ordered fragments examined were 36, 37, and 38. This yields an overall range of *n* of 36 to 50 corresponding to a composition range of $(Ta,W)O_{2.944}$ to $(Ta,W)O_{2.96}$ for the {103} *CS* phases. The small number of fairly well ordered fragments examined from the samples heated at 1673K all fell within this range and were in no way exceptional.

High-resolution electron microscope lattice images of {103} *CS* phases from samples prepared at 1623K revealed that the {103} *CS* planes were generally straight and formed relatively well-ordered arrays. Apart from the fact that the spacing between the *CS* planes was wider than in the binary tungsten oxides, the microstructures of the {103} *CS* regions seemed very similar. As such microstructures have been well illustrated in the past (*8*), they will not be described further here. In addition to the *CS* arrays, in samples with compositions fairly close to WO_3, isolated {103} *CS* planes, or small groups of such features, were observed. As these faults do not occur in the binary W–O system, similar examples are shown in Fig. 10.

Lattice images of {103} *CS* phases from samples prepared at 1673K showed a slightly different distribution of microstructures, in which ordered arrays of straight {103} *CS* planes were less frequently encountered and fragments containing isolated and small groups of *CS* planes lying on several sets of {103} *CS* planes were quite common. Typical examples of this sort of microstructure are shown in Fig. 10.

The X-ray results were in accord with

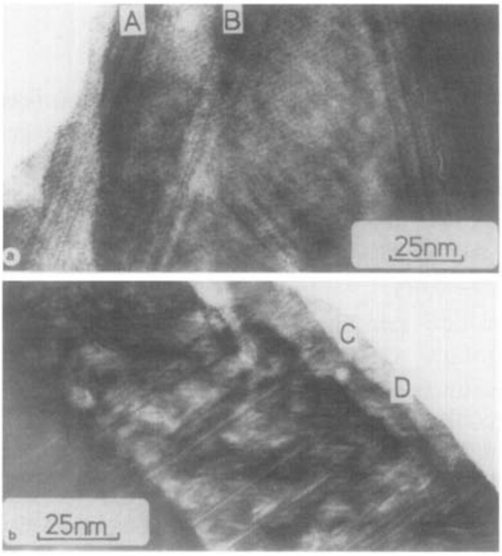

FIG. 10. Electron micrographs showing isolated {103} *CS* planes with microstructures similar to that shown by crystals containing a low density of {102} *CS* planes. In (a) the separation between the *CS* planes in each group is about 0.5 nm and between the groups A and B it is about 2.2 nm. In (b) the separation between the *CS* planes at C and D is about 2.0 nm.

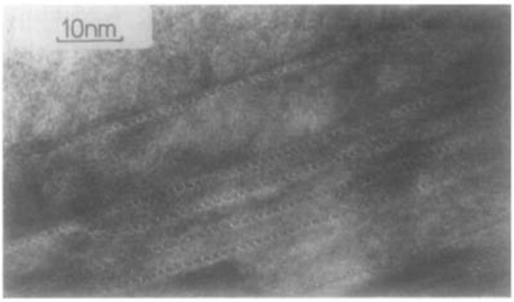

FIG. 11. Electron micrograph of a group of isolated {104} *CS* planes in a sample of overall composition $(Ta,W)O_{2.90}$. The *CS* planes also sometimes contain blocks of six edge-sharing octahedra characteristic of {103} *CS* planes.

these observations, and confirmed the narrow extension of the {103} *CS* structure field. For example, the $(Ta,W)O_{2.925}$ sample gave an X-ray powder pattern showing weak lines from a *TTB* structure as well as {103} *CS* lines, while the $(Ta,W)O_{2.975}$ samples showed faint WO_3 lines in addition to the {103} *CS* lines.

{104} CS Phases

In samples prepared at lower temperatures there was no evidence at all to suggest that {104} *CS* planes could form in this system. However, in preparations above 1623K the situation changed, and in samples heated at 1673K with compositions of $(Ta,W)O_{2.90}$ and $(Ta,W)O_{2.925}$ a few crystals which contained {104} *CS* planes were found. One fragment contained a well-ordered array of {104} *CS* planes. The composition of the flake, calculated from the diffraction pattern, was close to $(Ta,W)_{65}O_{192}$, i.e., $(Ta,W)O_{2.954}$. Some fragments with well-separated {104} *CS* planes were also found as shown in Fig. 11. We should note here that although {104} *CS* planes are well known in the niobium–tungsten oxides they have not been reported in the tantalum–tungsten oxide system before. Some effort was therefore put into checking the purity of the crystals and in particular they were analyzed for niobium, but always with negative results.

Wavy CS Structures

The wavy *CS* structures found in the Ta_2O_5–WO_3 system are not so pronounced as those occurring in the Nb_2O_5–WO_3 system, and the microstructures found seem to depend upon temperature of sample preparation in quite a marked fashion. In samples heated at 1623K only the $(Ta,W)O_{2.975}$ preparation contained crystals which included wavy *CS* structures. These were found in small numbers along with {102} *CS* in largely unfaulted WO_3. The wavy *CS* surfaces consisted of disordered {102} *CS* planes containing small numbers of blocks of six edge-sharing octahedra corresponding to units of {103} *CS* planes. Diffraction patterns obtained from fragments containing these structures showed only streaking along {102} directions and the true microstructures present in the crystals could only be deduced from high-resolution electron micrographs.

In samples prepared at 1673K, a different type of wavy *CS* structure was found. These wavy *CS* structures coexisted with fragments containing ordered arrays of {103} *CS* planes at the lower end of the phase range rather than at the upper end, as in the structures just described. Thus the $(Ta,W)O_{2.925}$ and $(Ta,W)O_{2.90}$ preparations were found to contain, in addition to the ordered {103} arrays reported above, the wavy microstructures shown in Fig. 12. These defects were found to consist of {103} *CS* planes which contained blocks of edge-sharing octahedra corresponding to units of {104} *CS* planes, and more rarely units of {102}, {105}, and {107} *CS* planes. The waves were rather irregular with no definable wavelengths. Diffraction patterns obtained from such crystal fragments only indicated that {103} *CS* was present, and as with the group mentioned above, only high-

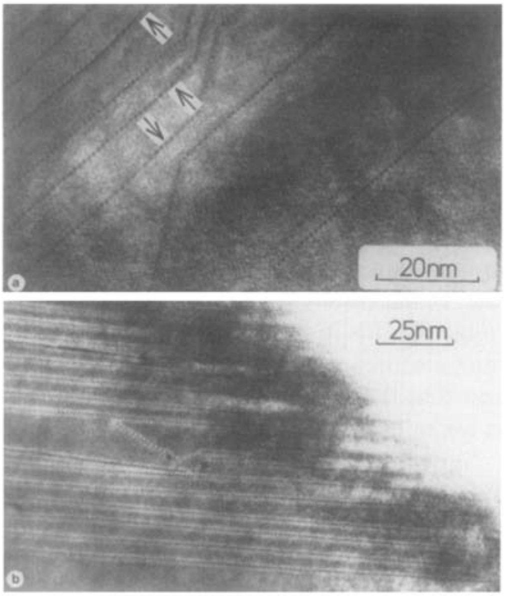

FIG. 12. Electron micrographs of wavy *CS* planes in Ta_2O_5–WO_3 samples heated at 1673K. In (a) regions of *CS* made up of units of eight edge-shared octahedra in mainly {103} *CS* planes are shown by arrows. In (b) regions of {102} and {104} *CS* occur in mainly {103} *CS*. This is best seen when the micrograph is viewed at grazing incidence. Both crystal fragments were taken from a sample of overall composition 0.1 Ta_2O_5 : $0.8WO_3$.

resolution micrographs were able to reveal the true complexity of the system.

{102} CS Planes

Crystal fragments containing disordered {102} *CS* planes were found in the $(Ta,W)O_{2.975}$ and $(Ta,W)O_{2.95}$ preparations heated at 1623K. The microstructures of these fragments were similar in appearance to those found in slightly reduced WO_3 and contained isolated or small groups of up to about six {102} *CS* planes in wide regions of unfaulted WO_3. As these microstructures have been illustrated in the past (*7*, *8*), micrographs will not be included here. X-Ray powder diffraction analysis of samples close to WO_3 in composition revealed a mixture of the monoclinic and orthorhombic WO_3 phases, which also suggested that a {102} *CS* structure field extended somewhat from the stoichiometric WO_3 oxide (*1*, *9*).

Discussion

In the Nb_2O_5–WO_3 system the dominant *CS* plane types were {104} and {001}. Although some {102} *CS* was found this does not occur over any appreciable composition range, and is possibly an artifact due to the preparation methods used. With this in mind, then, we find that the Nb_2O_5–WO_3 system makes use of neither {102} nor {103} *CS* planes to accommodate the loss of oxygen in the WO_3-like parent structure at 1600K. In the Ta_2O_5–WO_3 system the results are different than those in the Nb_2O_5–WO_3 system, and are far more similar to that found in the binary system. The major *CS* plane type here is {103}, although, once again, small amounts of {102} *CS* are found in some crystals, and at higher temperatures {104} *CS* starts to appear.

In the Nb_2O_5–WO_3 system the {104} *CS* range occupies a composition range of from $(Nb,W)O_{2.942}$ to $(Nb,W)O_{2.954}$, corresponding to the oxides $(Nb,W)O_{52}O_{153}$ to $(Nb,W)_{65}O_{192}$. This is in good agreement with the results of Allpress (*3*), who recorded a range from $n = 54$ to 63, and Bursill and Hyde (*4*), who recorded a range from $n = 56$ to 63. It is clear, therefore, that the reaction of Nb_2O_5 and WO_3 in the phase range that we are considering does not produce low densities of {104} *CS* planes in WO_3 which gradually increase in number, but instead we have a fairly precise upper boundary to the {104} *CS* plane range, which then coexists with WO_3 itself. In effect we have, at the upper composition end, a "two-phase" equilibria between WO_3 and the {104} *CS* series. The same is true in the Ta_2O_5–WO_3 system. Here we have a "two-phase" equilibria between WO_3 and {103} *CS* phases with compositions close to

$(W,Ta)_{50}O_{148}$, at least at temperatures on the order of 1623K.

This behavior suggests that neither the Nb nor the Ta atoms or ions are entering the WO_3 structure at random, but are segregating within the *CS* planes, for if this did not occur, behavior identical to that in the binary system would be expected. Allpress, in fact, made some progress toward quantitatively estimating the degree of segregation for some Nb_2O_5–WO_3 *CS* phases and showed that the amount of Nb within the *CS* planes was much higher than that occurring if a random distribution of atoms held (*3*). No data exists for the Ta_2O_5–WO_3 oxides, but recent studies on a $(Mo,W)_{14}O_{41}$ *CS* oxide revealed a segregation of Mo in the *CS* planes (*11*). The phenomenon could well be a general one, and is of some interest from a theoretical point of view. The difficulty in investigating this lies in the disordered nature of the crystals usually produced. It may, therefore, be worth putting some effort into careful crystal growth techniques in an attempt to produce well-ordered phases suitable for precise structure determination.

In both the Ta_2O_5–WO_3 and Nb_2O_5–WO_3 systems, addition of the pentavalent cation leads to the formation of a series of *CS* structures. A question of some interest is whether all of the substoichiometry is taken up by *CS* planes, or whether a "solid-solution" region exists in which the M^{5+} cations are incorporated into the WO_3 structure and balanced by some sort of point defect counter-defects. Very few of the previous studies use structural techniques which are able to discriminate between the various possibilities. Allpress (*3*), however, using electron microscopy and X-ray diffraction, which are structurally sensitive techniques, suggested that a solid-solution region existed in the Nb_2O_5–WO_3 region for the lowest concentrations of Nb_2O_5.

Our results allow us to comment upon this problem. The answer must be couched in experimental terms. In all of our preparations, *CS* phases were present. Certainly, *CS* planes were not found in each crystal flake examined, but even in preparations very close in composition to WO_3, use of optical microscopy for manual crystal selection followed by X-ray diffraction and electron microscopy left no doubt that each preparation did contain some *CS* material. Our results indicate that no solid-solution range obtains in the systems studied here at temperatures on the order of 1600–1700K and that the change in oxygen : metal ratio is taken up by *CS* formation.

Superficially the Nb_2O_5–WO_3, Ta_2O_5–WO_3, and WO_3 systems all behave rather differently with respect to the *CS* planes used in accommodating oxygen loss. However, this difference in behavior may not be as pronounced as appears at first sight. The most significant result, in this respect, is the observation that a change in preparation temperature of only 50°C in the Ta_2O_5–WO_3 preparation leads to the previously unsuspected formation of {104} *CS* planes. This observation is in agreement with a few previous results. Allpress (*3*), in his study of the Nb_2O_5–WO_3 system, indicated that {104} *CS* planes are preferred to {001} *CS* planes as the temperature rises. Thus in a sample of composition $Nb_2O_5 : 11WO_3$ ($MO_{2.023}$) prepared at 1552 to 1584K only {001} *CS* was found, while in a sample of the same composition heated at 1585K a good deal of {104} *CS* occurred. The same trend can be seen in his samples of composition $Nb_2O_5 : 15WO_3$. We can also note that Bursill and Hyde (*4*) reported that {105} *CS* phases could occur in the Nb_2O_5–WO_3 system, a fact which may also reflect variations in preparation temperature.

In order to compare *CS* structures in a meaningful way, it is now clear that phase relations over as wide a range of temperature as possible must be obtained, and that these temperatures must be controlled with precision. Any reinvestigation should also include the binary W–O system itself. To date, the highest temperatures at which preparations have been made in this latter system are close to 1473K. Experiments at temperatures of 1673K are of some interest and are already underway. Ideally, therefore, precise comparison of *CS* behavior in all these systems must be postponed until such data is available.

In a number of systems a composition region exists over which the *CS* planes change from one orientation to another. In some of these, the Cr_2O_3–TiO_2 oxides, for example, every composition within this phase interval leads to an ordered array of *CS* planes, the indices of which lie somewhere between the two extremes. This situation is referred to as a swinging *CS* plane region. In our study this type of microstructure does not occur, at least at the temperatures we employed in our preparations. In the Nb_2O_5–WO_3 system a swinging *CS* plane region could be expected to form between the {104} and {001} *CS* types, but instead we get an intergrowth between the two types. The intergrowth has remnants of order, but this is not as significant as the ordering which occurs in the swinging *CS* phases.

There are a number of points to comment on with respect to this region in the Nb_2O_5–WO_3 system. The first of these concerns the spacings of the bottom member of the {104} series, $(Nb,W)_{52}O_{153}$, and the upper member of the {001} series, $(Nb,W)_{16}O_{47}$. It is a straightforward matter to calculate the idealized distance between *CS* planes in these arrays, using formulae which have been given in the past (*3*, *4*, *8*). We find that the spacings are very close to one another. In fact the spacing of the {104} *CS* planes in $(Nb,W)_{52}O_{153}$ corresponds exactly to the spacing of the {001} *CS* planes in $(Nb,W)_{13}O_{38}$, and the spacing of the {001} *CS* planes in $(Nb,W)_{16}O_{47}$ to the spacing of the {104} *CS* planes in $(Nb,W)_{65}O_{192}$. Within the experimental error associated with determination of the phase ranges of the *CS* compounds we see that the spacing of the *CS* planes at the bottom of the {104} *CS* range is equal to the *CS* spacing at the top of the {001} *CS* range. It thus appears that when the {104} *CS* plane set transforms to the {001} set, the *CS* plane spacing does not change significantly. This feature seems to be a common one in *CS* systems, where one *CS* type changes to another. It may well reflect the high energy that would be associated with the incoherent boundary which would form between regions of differing *CS* spacing where they adjoined.

Another point concerns the nature of the intergrowth itself. Although extensive regions of {104} *CS* are sometimes found to join to regions of {001} *CS*, this is not usual, and instead some sort of wavy *CS* structure is found. This is a very variable microstructure but the wave amplitudes and wavelengths probably vary with niobium composition. The actual wave structure seems to represent an attempt by the crystals to minimize elastic strain, as similar waves in rutile oxides have been shown to arise in this way (*12*). Unfortunately the elastic constants of WO_3 are unknown, and exact calculations to confirm the elastic strain hypothesis are not possible at this time.

Acknowledgments

T. E. is grateful to Professor Arne Magnéli and to the Swedish Natural Science Research Council for support of this study. P. E. thanks the Science Research Council, London, for financial support.

References

1. T. Ekström and R. J. D. Tilley, *J. Solid State Chem.* **18**, 123 (1976).

2. R. S. Roth and J. L. Waring, *J. Res. Nat. Bur. Stand. A*, **70** 281 (1966).

3. J. G. Allpress, *J. Solid State Chem.* **4**, 173 (1972).

4. L. A. BURSILL AND B. G. HYDE, *J. Solid State Chem.* **4,** 430 (1972).
5. P. GADÓ, B. HOLMBERG, AND A. MAGNÉLI, *Acta Chem. Scand.* **19,** 2010 (1965).
6. P. GADÓ AND A. MAGNÉLI, *Mater. Res. Bull.* **1,** 33 (1966).
7. T. EKSTRÖM AND R. J. D. TILLEY, *Chem. Scr.* **16,** 1 (1980).
8. R. J. D. TILLEY, *Chem. Scr.* **14,** 147 (1978–79).
9. J. BOOTH, T. EKSTRÖM, E. IGUCHI, AND R. J. D. TILLEY, *J. Solid State Chem.* **41,** 293 (1982).
10. M. SUNDBERG, T. EKSTRÖM, AND R. J. D. TILLEY, in preparation.
11. K. VISWANATHAN AND E. SALJE, *J. Solid State Chem.*, in press.
12. L. A. BURSILL, D. J. NETHERWAY, AND I. E. GREY, *Nature (London)* **272,** 405 (1978).